Liquid Crystals
Publication details, including instructions for authors and subscription information:
http://www.informaworld.com/smpp/title~content=t713926090

Possibility of isostructural condensed states of matter in the D phase of ANBC and the cubic mesophase of BABH: heat capacity of 4'-*n*-octadecyloxy-3'-nitrobiphenyl-4-carboxlic acid, ANBC(18)

Ayako Sato; Yasuhisa Yamamura; Kazuya Saito; Michio Sorai

Online publication date: 06 August 2010

To cite this Article Sato, Ayako , Yamamura, Yasuhisa , Saito, Kazuya and Sorai, Michio(1999) 'Possibility of isostructural condensed states of matter in the D phase of ANBC and the cubic mesophase of BABH: heat capacity of 4'-*n*-octadecyloxy-3'-nitrobiphenyl-4-carboxlic acid, ANBC(18)', Liquid Crystals, 26: 8, 1185 — 1195
To link to this Article: DOI: 10.1080/026782999204219
URL: http://dx.doi.org/10.1080/026782999204219

LIQUID CRYSTALS, 1999, VOL. 26, NO. 8, 1185–1195

Possibility of isostructural condensed states of matter in the D phase of ANBC and the cubic mesophase of BABH: heat capacity of 4′-*n*-octadecyloxy-3′-nitrobiphenyl-4-carboxlic acid, ANBC(18)†

AYAKO SATO, YASUHISA YAMAMURA, KAZUYA SAITO
and MICHIO SORAI*
Microcalorimetry Research Center, School of Science, Osaka University,
Toyonaka, Osaka 560-0043, Japan

(*Received 12 January 1999; accepted 23 February 1999*)

Heat capacity measurements have been made on ANBC(18) at temperatures from 8 to 490 K by adiabatic calorimetry. All known phases were detected. The temperatures, enthalpies and entropies of transition were determined for the phase transitions observed. On the basis of the entropy of transition to the SmC phase from the D or cubic phases, it is pointed out that the D phase of ANBC and the cubic phase of BABH might be identical in nature. It is shown that the arrangement of 'molecular' cores has a higher degree of *order* in the isotropic (D and cubic) phases than in the SmC phase, whereas the terminal alkoxy chains are more *disordered* in the isotropic phases than in the SmC phase. The degrees of disorder in the D and cubic phases relative to the SmC phase are very similar in terms of the entropy of transition per methylene group. The inverted phase sequence in ANBC (SmC → D on heating) and BABH (cubic → SmC) can be accounted for in terms of the competing roles in the entropy between the molecular core and the chains.

1. Introduction

The D phase of ANBC(n_C) (4′-*n*-alkoxy-3′-nitrobiphenyl-4-carboxylic acid, n_C = the number of carbon atoms in the alkoxy chain) belongs to an interesting class of liquid crystals because of its isotropic nature [1–3]. The molecule of ANBC consists of a nitrobiphenylcarboxylic acid core and an *n*-alkoxy chain as shown in figure 1. Since most molecules are dimerized in the solid and liquid crystalline phases [4, 5] owing to intermolecular hydrogen bonds, the system consists of a 'molecule' that has a long core at its centre and two terminal alkoxy chains.

Another isotropic liquid crystal called 'cubic phase' was discovered in 1981 [6, 7] in a series of BABH(n_C) [1,2-bis(4-*n*-alkoxybenzoyl)hydrazine], the molecular structure of which is also shown in figure 1. In contrast to ANBC, the BABH molecule has a 'dimerized or doubled' structure even in the isolated state. Although the similarity in the 'molecular' structure and the isotropic nature of both the phases naturally lead to an expectation that the D phase of ANBC and the cubic phase of BABH are identical, the expectation has been denied by the results of miscibility tests [7]. Specifically, there exists an immiscible region in which these two mesophases do not merge. It has been, however, pointed out in a previous paper [8] that the result of the

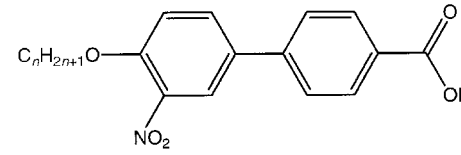

ANBC(*n*)

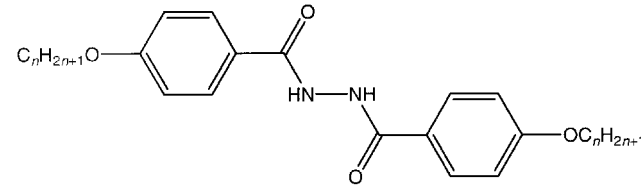

BABH(*n*)

Figure 1. Structures of the ANBC and BABH molecules.

*Author for correspondence;
e-mail: sorai@chem.sci.osaka-u.ac.jp
†Contribution No. 159 from the Microcalorimetry Research Center.

Journal of Liquid Crystals ISSN 0267-8292 print/ISSN 1366-5855 online
http//www.tandf.co.uk/JNLS/lct.htm
http//www.taylorandfrancis.com/JNLS/lct.htm

miscibility test cannot necessarily stand as evidence for the different nature of these two mesophases with inverted phase sequences (SmC → D in ANBC and cubic → SmC in BABH on heating). The question is thus open at present as to whether the D and cubic phases are identical or not.

In addition to its isotropic nature, study of the D phase reveals another interesting aspect. Different parts of the molecules play different roles as evidenced by the study of the binary system ANBC–*n*-tetradecane [9]. The terminal alkoxy chains behave in the D phase like a solvent as in the case of lyotropic liquid crystals. In the present paper, discussion will be extended along this line.

The widely accepted structural model for the D phase is the so-called interwoven jointed-rod model [10–14], proposed first by Tardieu and Billard [10]. The model is consistent with X-ray diffraction [10–14], NMR [5, 15] and dynamic viscoelastic measurements [16]. The establishment of the structural model prompts construction of molecular (statistical) models of the peculiar aggregation style of molecules such as those in the D phase. Since reliable thermodynamic data are crucial to proposing a concrete framework for possible statistical models and to discriminating good statistical models, the present authors began their thermodynamic studies on thermotropic liquid crystalline phases with isotropic symmetry [8, 9, 17].

In the first paper in this series of studies [9], the phase diagrams of the binary systems, ANBC(n_C)–*n*-tetradecane (n_C = 8, 16 and 18) were studied while paying special attention to the roles of the molecular core and terminal chains in relation to the thermodynamic stability of the D phase. The results show that the apparent dependence of the effective number of paraffinic carbon atoms in the system resembles the n_C dependence in the homologous series of ANBC(n_C), implying that the terminal alkoxy chains in, at least, the D phase behaves like a solvent just as in the case of lyotropic liquid crystals. The minimum effective size of the 'molecular core' required for stabilizing the D phase was also suggested.

The second paper [17] is concerned with the thermodynamic properties of BABH(8). The results show that the entropy of transition between the cubic and SmC mesophases is very small in spite of a large difference in their structures.

The results of precise heat capacity measurements were reported in the third paper on ANBC(16) [8]. It was shown that the small entropy of transition between the layered SmC and the isotropic liquid crystalline phases is a common property of both ANBC(16) and BABH(8).

This paper describes experimental detail and results of precise adiabatic calorimetry on ANBC(18). The phase sequence of the ANBC(18) on heating is as follows [1, 18]: room temperature crystal–high temperature crystal–SmC phase–D phase–isotropic liquid. Through a thermodynamic argument based on the entropy of transition, the possibility will be pointed out that the D phase of ANBC and the cubic phase of BABH may be identical in nature. The core of the argument is based on the fact that the SmC phase neighbours the isotropic phase in both ANBC and BABH. Since entropy is a measure for the possible number of microscopic states, direct comparison of entropy between different compounds provides us with a useful clue for interpretation of the nature of the isotropic phases. Unless the order in the relevant degrees of freedom changes appreciably between the SmC and the isotropic phases, the entropy of transition directly reflects the change in the degrees of freedom, irrespective of the transition temperature.

2. Experimental

The specimen of ANBC(18) was synthesized according to the method reported [1] starting from 4′-hydroxybiphenyl-4-carboxylic acid (Aldrich Chemical), 1-bromooctadecane (Wako Pure Chemicals) and fuming nitric acid (Wako Pure Chemicals), and purified by repeating crystallization from ethanol. The quality of the specimen was checked by elemental analysis, ^{1}H NMR, and mass spectrometry; no impurities were indicated. The purity of the sample used for calorimetry was finally determined as 99.0 mol % by the factional melting method described below. The sample was dried in a vacuum before loading into the calorimeter vessel.

Two adiabatic calorimeters were used for heat capacity measurements, one below and one above room temperature. For measurements below room temperature made by calorimeter A [19], 1.7956 g (3.509 mmol) of sample after buoyancy correction were loaded into a gold-plated copper calorimeter vessel together with helium gas (100 kPa) at room temperature to assist thermal equilibration within the vessel. The working thermometers attached to the calorimeter vessel were platinum (Minco Product, S1055) and germanium (Lake-Shore Cryotronics, GR-200B-500) resistance thermometers. Their temperature scales are based on ITS-90. Measurements were carred out down to 8 K. The sample contributed more than 25% to the total heat capacity including that of the calorimeter vessel throughout the temperature range studied. The details of the adiabatic calorimeter, the operation and the procedure for heat capacity measurement have been described in detail elsewhere [19].

For the measurements above room temperature using the calorimeter B [20], 2.9989 g (5.861 mmol) of sample were loaded into a quartz glass beaker with a lid (5.7 g in mass), to avoid direct contact between the sample

and the wall of the gold-plated copper–beryllium vessel. The beaker was put in the vessel and sealed with a small amount of helium gas (23 kPa at room temperature). The thermometer mounted on the calorimeter vessel was a platinum resistance thermometer (Minco Product, S1059), of which the temperature scale is based upon IPTS-68. The contribution of the sample was more than 20% of the total heat capacity including the vessel and the glass beaker. The details of the adiabatic calorimeter, the operation and procedure of heat capacity measurement have been described in detail elsewhere [20].

The difference between the ITS-90 and IPTS-68 is significant and irregular at low temperatures while it is small and smooth above room temperature up to about 600 K [21]. The heat capacities determined by the two calorimeters have not been adjusted by correcting IPTS-68 to ITS-90 in the present paper.

To establish the temperature dependence of the heat capacity above the transition to the isotropic liquid, a commercial DSC instrument (Perkin-Elmer, DSC-7) was employed because adiabatic calorimetry was so time consuming (about 70 min per data point) that the sample decomposes slowly at high temperatures. In contrast, DSC made at a rapid scan rate (5 K min^{-1}) gave completely reproducible thermograms, implying no decomposition.

3. Results and discussion

3.1. *Heat capacity, excess enthalpy and entropy, and thermodynamic functions*

The heat capacity of ANBC(18) was measured between 8 and 480 K by adiabatic calorimetry. The time required for thermal equilibration was within 3 min below 30 K, 5 min at 100 K, 7 min at 200 K and 8 min at 300 K for calorimeter A. The time was about 30 min at 300 K for calorimeter B outside the transition region. In the transition region, the thermal relaxation time was significantly and abruptly prolonged as the transition temperature was approached. The longest time used for monitoring the temperature drift was, however, 120 min in these experiments for practical reasons. This truncation obviously has an influence on the resultant data for the apparent heat capacity, but no effect on the integrated enthalpy change because of the first law of thermodynamics. In reality, since the transitions are of first order, resulting in a narrow temperature interval where the time required for thermal equilibration is significantly longer than 120 min, the accuracy for the resultant excess enthalpy and entropy mostly depends on the uncertainty in drawing a baseline.

The primary data of the present heat capacity measurements are tabulated in table 1. The temperature increment due to each energy input may be deduced from the adjacent mean temperatures. Typical data are shown in figure 2 for the whole temperature range studied.

The largest anomaly due to the transition between the crystal and SmC phase (melting transition) was observed at 399.42 K with a latent heat of 42.50 kJ mol^{-1}. There seems no significant tail on either the low or high temperature sides. Using these quantities, determination of the purity of the sample was carried out by means of the fractional melting method, which utilizes the melting point depression. In the analysis, unknown impurities were assumed to be soluble in the liquid crystalline phase (SmC phase), but insoluble in the crystalline phase. The results of the analysis showed that the melting point of pure ANBC(18) is 399.79 K and the purity of the sample is 99.0 mol %.

Below the melting temperature there are two peaks and a broad hump in the heat capacity curve. While the sharp peak at 337.20 K is known to be due to a phase transition between crystalline phases [18], the other two anomalies are new in the present experiment. The sharp peak is attributed to a phase transition of the first order as judged from the abrupt increase in the time required for equilibration upon approaching the transition temperature. Although the peak at 324.82 K is extremely small, it may also be attributed to a phase transition between crystalline phases. The tail of this anomaly on the low temperature side seems to extend down to about 200 K. In what follows, these three crystalline phases will be designated as Cr_1, Cr_2 and Cr_3 on going from high to low temperature. The broad hump appearing in Cr_1 phase remained unchanged, after drying at 380 K for an hour, in the DSC experiments. This implies that the hump does not have an extrinsic origin such as solvent occluded in the sample, but is intrinsic. The hump has its maximum at 372 K.

To discuss the thermodynamic properties of transitions such as excess enthalpy and entropy, separation of the excess part is necessary. When a transition is of the first order, the normal heat capacity may jump at the transition temperature. It is, however, often hard to draw such a baseline for each phase. In the present case, a jump in the heat capacity due to different baselines is clearly recognized for the transition at 337.20 K. The baseline of the heat capacity below this temperature, i.e. phases Cr_3 and Cr_2, was determined by using the effective frequency distribution method [22]. The resultant normal heat capacity is shown by the solid curve in figure 2. For Cr_1, the heat capacity of the SmC phase fitted to a quadratic polynomial was extrapolated. The excess heat capacities thus separated from the observed heat capacities were integrated numerically to yield the excess enthalpy and entropy. The numerical data are given in table 2 and the temperature dependence of

Table 1. Measured molar heat capacities of ANBC(18).

T/K	$C_{p,m}$/J K^{-1} mol^{-1}	T/K	$C_{p,m}$/J K^{-1} mol^{-1}	T/K	$C_{p,m}$/J K^{-1} mol^{-1}	T/K	$C_{p,m}$/J K^{-1} mol^{-1}
Series A-1		189.040	475.59	13.903	19.317	60.971	189.90
96.312	290.49	191.171	479.83			62.160	193.88
97.602	293.62	193.291	483.95	*Series A-3*		63.359	197.75
98.904	296.72	195.403	488.07	14.494	21.107	64.548	201.67
100.221	300.00	197.529	491.88	15.041	22.848	65.728	205.24
101.552	303.22	199.668	496.30	15.597	24.700	66.923	209.10
102.896	306.20	201.796	500.92	16.166	26.200	68.150	213.03
104.254	309.27	203.939	504.83	16.746	27.879	69.392	216.73
105.636	312.40	206.149	509.09	17.337	29.221	70.629	220.75
107.041	315.69	208.458	514.04	17.931	31.157	71.871	224.33
108.463	318.85	210.809	518.62	18.523	33.234	73.127	227.99
109.900	322.10	213.212	523.39	19.113	35.091	74.393	231.76
111.371	325.42	215.653	528.33	19.702	36.830	75.658	235.36
112.878	328.40	218.081	533.70	20.288	38.883	76.918	239.06
114.403	331.83	220.526	538.93	20.877	41.319	78.179	242.59
115.947	335.50	222.989	544.45	21.486	42.734	79.443	246.13
117.511	338.62	225.452	549.40	22.123	45.147	80.715	249.74
119.107	342.07	227.902	555.42	22.783	47.455	81.993	253.22
120.719	344.89	230.339	559.37	23.463	50.086	83.264	256.67
122.317	348.52	232.762	566.30	24.161	53.457	84.528	260.17
123.902	351.95	235.237	570.41	24.881	55.636	85.791	263.46
125.475	355.03	237.760	577.41	25.622	59.262	87.073	266.88
127.037	358.16	240.269	582.81	26.378	61.552	88.367	270.18
128.586	361.28	242.764	589.01	27.146	64.822	89.658	273.52
130.123	364.50	245.243	596.20	27.926	67.745	90.957	276.86
131.709	367.96	247.771	602.34	28.721	70.810	92.265	280.24
133.308	370.85	250.344	608.52	29.537	73.468	93.571	283.49
134.862	373.96	252.905	615.25	30.368	77.554	94.864	286.70
136.407	376.96	255.449	623.02	31.197	80.947	96.152	289.84
137.943	379.72	257.979	629.36	32.034	83.081	97.432	293.04
139.523	382.76	260.555	636.35	32.874	87.486	98.702	296.17
141.148	385.99	263.174	643.90	33.716	90.117	99.960	299.29
142.762	388.93	265.779	651.19	34.571	93.003		
144.366	392.22	268.368	658.57	35.439	96.365	*Series B-1*	
145.961	395.11	270.941	665.73	36.270	99.512	253.643	620.27
147.600	398.18	273.559	673.70	37.069	102.75	255.821	625.81
149.281	401.80	276.218	681.72	37.906	106.06	257.989	631.83
150.953	404.59	278.858	690.39	38.796	109.21	260.148	638.62
152.615	407.60	281.483	699.65	39.748	113.01	262.298	644.75
154.268	410.69	284.044	708.08	40.732	116.93	264.439	650.70
155.963	413.68	286.579	716.97	41.724	120.76	266.572	657.62
157.699	416.81	289.209	727.27	42.728	124.45	268.658	664.20
159.426	420.03	291.965	735.35	43.730	128.31	270.700	669.93
161.145	423.19	294.790	746.58	44.726	131.98	272.872	676.41
162.853	426.28	297.643	758.05	45.722	135.70	275.171	683.27
164.603	429.79	300.513	770.33	46.727	139.32	277.455	690.96
166.395	432.87			47.747	143.01	279.723	698.82
168.176	436.18	*Series A-2*		48.783	147.03	281.980	706.61
169.949	439.67	8.874	7.817	49.832	150.93	284.232	711.54
171.712	443.08	9.277	8.519	50.888	154.87	286.479	721.04
173.516	446.20	9.707	9.347	51.947	158.31	288.708	731.94
175.352	449.79	10.169	10.258	53.011	162.59	291.178	738.62
177.195	452.96	10.667	11.222	54.085	166.47	293.908	742.78
179.071	456.55	11.187	12.621	55.180	170.12	296.657	754.34
180.979	460.17	11.727	13.829	56.302	174.28	299.408	767.06
182.921	464.09	12.282	14.843	57.452	178.29	302.144	779.06
184.898	467.54	12.851	16.321	58.619	182.10	304.871	790.11
186.934	471.15	13.399	17.669	59.794	185.99	307.588	804.95

Table 1. (*Continued*).

T/K	$C_{p,m}$/J K^{-1} mol^{-1}	T/K	$C_{p,m}$/J K^{-1} mol^{-1}	T/K	$C_{p,m}$/J K^{-1} mol^{-1}	T/K	$C_{p,m}$/J K^{-1} mol^{-1}
310.292	819.37	337.883	2169.3	397.931	6605.8	427.996	3667.7
312.981	833.56	339.133	1111.8	398.380	10713	428.150	3559.6
315.656	849.25	340.548	1014.9	398.697	16347	428.334	1761.0
318.314	867.11	341.981	1005.4	398.926	23161	428.559	1172.2
320.258	881.32	343.415	1010.4	399.097	31432	429.167	1168.0
321.503	896.90	344.846	1016.4	399.231	39986	430.141	1166.6
322.741	915.68	346.393	1024.0	399.338	50521	431.632	1175.2
323.968	956.03	348.053	1031.7	399.423	64224	433.637	1182.3
325.302	990.00	349.458	1039.4	399.531	33699	435.638	1187.4
326.749	992.52	350.444	1044.3	400.193	1234.9	437.636	1196.3
328.066	1001.1	351.182	1049.4	401.411	1125.3	439.630	1202.8
329.251	1020.4	351.836	1050.7	402.636	1125.9	441.622	1209.9
330.428	1041.6	352.491	1053.4	404.423	1129.4	443.611	1217.9
331.597	1070.4	353.144	1060.7	406.772	1134.6	445.597	1224.5
332.850	1124.7	353.797	1061.0	409.321	1137.6	447.581	1230.9
334.171	1232.0	354.449	1065.6	412.069	1142.6	449.563	1241.1
335.428	1535.5	355.100	1070.2	414.814	1149.8	451.542	1246.1
336.557	2186.9	355.750	1071.9	417.553	1159.3	453.521	1253.5
337.602	2208.5	356.479	1076.2			455.497	1259.5
338.771	1264.9	357.487	1085.1	*Series B-3*		457.472	1270.8
340.101	1050.5	358.990	1092.9	402.743	1129.6	459.445	1289.1
341.470	1021.1	360.789	1102.6	404.847	1132.5	460.865	1289.6
342.845	1012.8	362.583	1111.0	406.946	1136.4	461.682	1305.7
344.220	1015.0	364.371	1119.3	408.627	1137.4	462.500	1313.2
345.593	1021.9	366.155	1125.3	409.892	1137.9	463.073	1307.7
346.964	1028.9	367.936	1131.4	411.017	1139.7	463.397	1288.4
358.894	1100.4	369.713	1136.6	412.004	1142.4	463.711	1518.6
361.506	1110.1	371.488	1139.0	412.990	1147.1	463.991	1754.3
364.110	1119.9	373.260	1142.1	413.976	1147.5	464.242	2277.8
366.706	1127.4	375.030	1142.3	414.961	1147.8	464.480	2850.2
369.295	1136.1	376.799	1143.7	415.946	1151.2	464.701	2799.5
371.878	1140.9	378.567	1144.3	416.930	1154.1	464.970	1654.9
		380.334	1142.1	417.913	1158.1	465.497	1640.0
Series B-2		382.101	1143.4	418.895	1156.2	466.261	1629.1
323.656	951.31	383.719	1143.3	419.877	1157.8	467.250	1654.4
324.457	997.35	385.188	1147.3	420.858	1160.4	468.462	1701.7
325.146	1001.7	386.659	1148.4	421.839	1163.8	469.666	1740.1
325.730	992.67	388.129	1154.8	422.819	1168.9	470.872	1744.1
326.315	989.64	389.595	1169.6	423.798	1169.1	472.087	1727.0
328.764	1022.9	390.920	1190.8	424.778	1171.6	473.752	1667.6
330.195	1044.3	392.102	1219.6	425.757	1172.6	475.904	1583.7
331.614	1078.1	393.270	1279.1	426.492	1175.4	478.129	1508.0
333.016	1137.0	394.413	1389.2	426.983	1179.1	480.431	1449.7
334.385	1256.2	395.496	1737.1	427.348	1165.3	482.806	1411.8
335.679	1610.7	396.482	2488.3	427.588	1174.6	485.260	1379.0
336.817	2451.6	397.305	3972.6	427.812	1695.3		

the transition entropy is shown in figure 3. Since the partition of the excess enthalpy and entropy gain between the two phase transitions occurring in the solid state was difficult, we treated them as a whole. The jumps in enthalpy (latent heat) and entropy roughly estimated for the higher transition at 337.20 K are 4.2 kJ mol^{-1} and 13 J K^{-1} mol^{-1}, respectively. It is hard to discuss at present the properties of each phase transition between the crystalline phases because information concerning the crystal structures and molecular dynamics in each phase is not available. However, it is plausible that since the molecule is too large to have an overall rotation, the large increment in enthalpy and entropy implies a successive conformational disordering of the terminal alkoxy chains. This point will be discussed later in some detail.

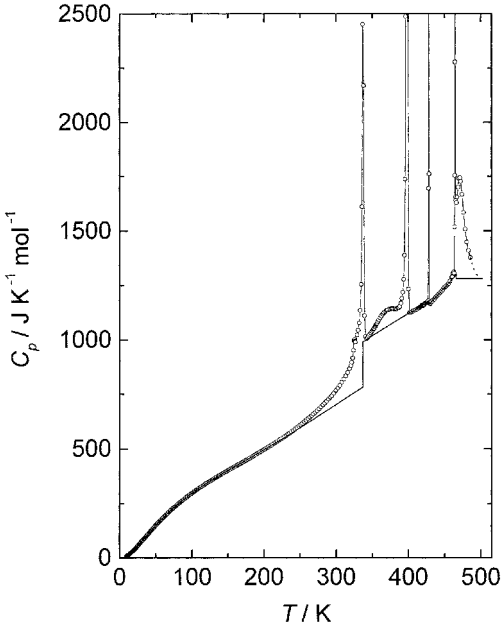

Figure 2. Measured molar heat capacities of ANBC(18) for the whole temperature region studied. The baselines to separate the excess heat capacities are drawn as solid curves.

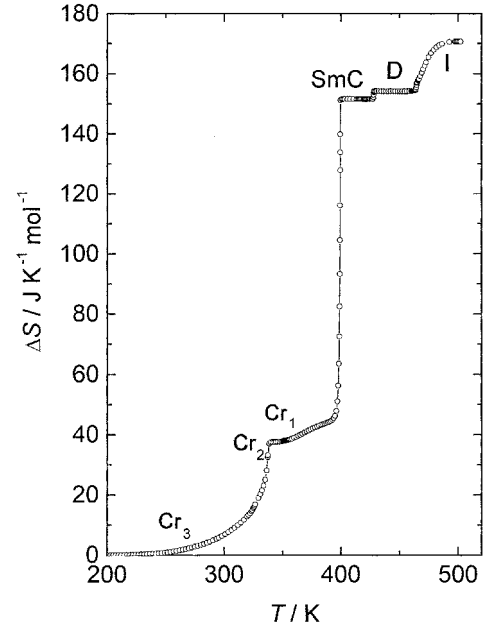

Figure 3. Temperature evolution of the excess entropy gain for ANBC(18).

Table 2. Thermodynamic quantities associated with phase transitions in ANBC(18).

Transition	T_{trs}/K	$\Delta_{trs}H$/kJ mol^{-1}	$\Delta_{trs}S$/JK^{-1} mol^{-1}
Cr_3–Cr_2	324.82	14.72	44.94
Cr_2–Cr_1	337.20		
Cr_1–SmC	399.42[a]	42.50	106.58
SmC–D	428.07	1.14	2.66
D–I	464.01	1.88	4.05

[a] Melting point of virtually pure ANBC(18) is 399.79 K.

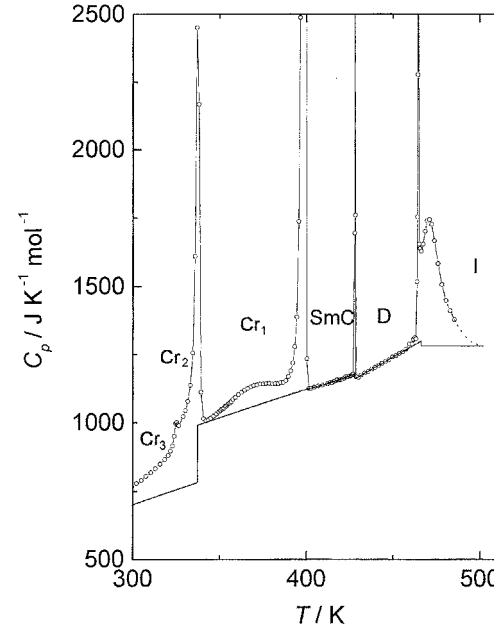

Figure 4. Measured heat capacities of ANBC(18) above room temperature. Extrapolation based on the DSC thermograms is shown by the dotted curve.

The heat capacity above 300 K is shown on an enlarged scale in figure 4. The transition temperature was determined as 399.42 K for the melting and 428.07 K for the first order SmC–D transition. The normal heat capacities for SmC and D phases were approximated by quadratic polynomials. The enthalpy and entropy gains were determined as 42.50 kJ mol^{-1} and 106.58 J K^{-1} mol^{-1} for the melting process, and as 1.14 kJ mol^{-1} and 2.66 J K^{-1} mol^{-1} for the inter-mesophase transition, respectively. The data are summarized in table 2 and the transition entropy is represented graphically in figure 3.

The heat capacity curve exhibits a hump in the isotropic liquid phase above 464.01 K. The existence of this hump has already been reported in the thermogram of a DSC experiment [18]. For the separation of this hump and the determination of the enthalpy and entropy of transition for the cubic D–isotropic liquid transition, heat capacity measurements in a higher temperature region are required to estimate the normal heat capacity in the isotropic liquid region. However, the sample slowly decomposed in measurements by adiabatic calorimetry because of the long exposure to heat. The temperature dependence of the heat capacity was thus determined by

DSC. Since the accuracy is much better in adiabatic calorimetry than in DSC, the heat capacity curve determined by adiabatic calorimetry was extrapolated as shown in figure 4 by the dotted curve, with reference to the DSC thermograms. We simply assumed the normal heat capacity in the isotropic liquid phase to be a temperature independent line shown in figure 4 to determine the excess thermodynamic quantities associated with the D–isotropic liquid transition and the hump appearing in the isotropic liquid. The enthalpy and entropy of transition are determined as 1.88 kJ mol^{-1} and 4.05 J K^{-1} mol^{-1}, respectively. Numerical integration of the hump gives excess enthalpy and entropy gains of 5.93 kJ mol^{-1} and 12.49 J K^{-1} mol^{-1}, respectively.

Standard thermodynamic functions of ANBC(18) were calculated by numerical integration of the present results, and are listed in table 3 at rounded temperatures. For the lowest temperature region, the heat capacity curve was extrapolated smoothly to 0 K.

3.2. *Hump of the heat capacity in the isotropic liquid phase*

The hump of heat capacity in the isotropic liquid region has been widely observed in the homologous series of ANBC(n_C) [18]. Similar broad humps have also been reported for some liquid crystalline substances at temperatures above that for destruction of a higher order structure, and the possibility of assignment of the hump to the destruction of a shorter range order than the original unit length has been suggested [23]. In the study on the binary system ANBC–*n*-tetradecane [9], the present authors pointed out the absence of the hump in the systems without a D phase, and reported the growth of the hump with increasing number of paraffinic carbon atoms in the binary systems between ANBC and *n*-tetradecane. This trend was interpreted by assuming that the hump is due to the dissociation of ANBC dimer and that the growth originates in the entropy effect. A comparison was made for ANBC(16) in ref. [8] between

Table 3. Standard thermodynamic functions of ANBC(18).

T / K	$C^\circ_{p,m}$ / J K^{-1} mol^{-1}	S°_m / J K^{-1} mol^{-1}	$[H^\circ_m(T)-H^\circ_m(0)]/T$ / J K^{-1} mol^{-1}	$-[G^\circ_m(T)-H^\circ_m(0)]/T$ / J K^{-1} mol^{-1}
10	9.90	4.02	2.92	1.10
20	37.90	18.81	12.93	5.88
30	75.80	41.17	27.43	13.74
40	113.9	68.22	44.31	23.91
50	151.6	97.73	62.04	35.69
60	186.7	128.5	79.94	48.6
70	218.6	159.7	97.50	62.2
80	247.7	190.9	114.5	76.4
90	274.5	221.6	130.8	90.8
100	299.3	251.8	146.4	105.4
120	343.8	310.4	175.7	134.7
140	283.8	366.5	202.6	163.9
160	421.2	420.2	227.6	192.6
180	458.4	471.9	251.2	220.7
200	497.0	522.2	273.8	248.4
220	537.7	571.5	295.9	275.5
240	582.8	620.1	317.9	302.2
260	636.2	668.8	340.2	328.5
280	697.3	717.9	363.3	354.6
300	768.9	768.3	387.8	380.5
320	879.4	821.1	414.8	406.3
			transition at 324.82 K	
			transition at 337.20 K	
340	1066.8	893.8	461.2	432.6
360	1105	953.5	493.6	459.9
380	1143	1014.6	527.1	487.5
			transition at 399.42 K	
420	1158	1235	686.9	549
			transition at 428.07 K	
440	1204	1293	711.8	581
460	1289	1348	734.8	613
			transition at 464.01 K	
480	1461	1417	771.4	645
298.15	761.2	763.5	385.4	378.1

the experimental and calculated heat capacities using the temperature evolution of the fraction of ANBC(16) molecules participating in dimer formation, the fraction having been determined from the signal intensity in the infrared spectra [4]. The results clearly showed that some cooperative mechanism must be involved to account fully for the hump. This is also the case of the present compound.

3.3. *Excess entropy and the conformational disorder of the terminal chain*

A large degree of supercooling amounting to 20 K was observed in the DSC experiments for the phase transitions from the cubic D phase to the SmC phase. Superheating was also observed for ANBC(16) [8]. These facts show that the structural reorganization between the layered structure of the SmC or SmA phase and the cubic structure of the D phase is a slow complicated process. Therefore, the D phase has a structure that is much different from those of the neighbouring smectic phases because supercooling and superheating phenomena are rarely observed for common liquid crystalline substances.

The study on the binary system of ANBC and *n*-tetradecane clearly showed that the terminal alkoxy chains in the D phase behave like a solvent in lyotropic liquid crystals [9]. The small entropy gain at the transition between the SmC and D phases therefore implies that a highly dynamical disorder of the molecular and/or intramolecular motions is established in both phases. This was confirmed by semi-quantitative argument for ANBC(16) [8].

Most ANBC(16) molecules are known to be dimerized in the liquid crystalline states and to dissociate in the isotropic liquid [4]. Although the degree of dimerization is unknown for ANBC(18), many molecules are expected to be dimerized. The entropy of melting due to the molecular core is, therefore, expected to be between the entropy of melting of biphenyl ($55\ J\ K^{-1}\ mol^{-1}$) and that of *p*-quinquephenyl ($65\ J\ K^{-1}\ mol^{-1}$) [24]. The contribution to the entropy of melting from methylene and methyl groups has been estimated as 10.31 and $3.78\ J\ K^{-1}\ mol^{-1}$, respectively, from the entropy of melting of *n*-alkanes [25]. The contribution of the alkoxy chains is thus calculated as $179\ J\ K^{-1}\ mol^{-1}$. The total sum is estimated at about $240\ J\ K^{-1}\ mol^{-1}$. The experimental entropy gain is $158.2\ J\ K^{-1}\ mol^{-1}$ at the clearing point. This is smaller by about $80\ J\ K^{-1}\ mol^{-1}$ than the calculated value assuming complete disordering. It is natural to imagine that the methylene groups near to the molecular core retain some order while those far from the core are highly disordered [9]. The difference between calculated and experimental entropy gains would reflect such a situation.

The experimental value of the transition entropy shows that the alkoxy chains, though not completely disordered, are highly disordered in the liquid crystalline phases, in accordance with the fact that the terminal alkoxy chain is highly disordered in the D phase and behaves like a solvent [9]. The entropy of transition is small for the transition between the liquid crystalline phases, and the entropy gain at the crystalline phase transitions has a significant magnitude. These features are also observed in ANBC(16) [8] and BABH(8) [17]. These facts suggest that potential disorder is necessary to stabilize and/or establish a complicated higher order structure with cubic symmetry consisting of long molecules as the building blocks.

3.4. *Role of the molecular core and the terminal alkoxy chain in SmC and cubic D phases*

The entropy of transition for the SmC–D transition in ANBC(18) ($2.66\ J\ K^{-1}\ mol^{-1}$) is larger than that in ANBC(16) ($1.63\ J\ K^{-1}\ mol^{-1}$) [8] by a factor of 1.6. Since the difference in molecular structure is small (only two methylene groups), it is hard to attribute the difference in the entropy of transition to that in molecular arrangement. An alternative way to interpret the difference should be considered. In the previous paper [9], the authors showed that the molecular core and the terminal chain play different roles in the SmC and cubic D phases. The analysis along this line seems to be acceptable because the difference is caused only by elongation of the chain. Although the transition entropies determined by adiabatic calorimetry are more accurate than those by DSC, the values of the transition entropies reported from DSC experiments are used for consistent comparison in the following discussion.

The entropies of transition from the SmC to D phases for the ANBCs [18] are plotted against the number of carbon atoms in the alkoxy chain (n_C) in figure 5. For the sake of comparison, the data determined by adiabatic calorimetry are also plotted in figure 5. A linear relation

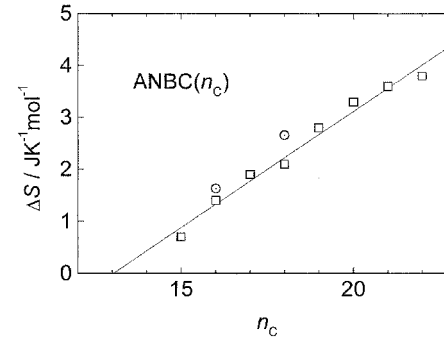

Figure 5. Entropy of transition between SmC and D phases in ANBC(n_C). Open squares, DSC data [18]: open circles, the present and previous [8] adiabatic calorimetry.

with a positive slope is recognized. This plot clearly shows that the conformational degrees of freedom of the alkoxy chain are relevant to this transition, and that the alkoxy chain has a higher degree of *disorder* in the D phase. The latter conclusion is consistent with the fact that the ^{1}H NMR signal is sharper in the D phase than in SmC phase [15].

The contribution of a methylene group is estimated as about 0.5 J K^{-1} mol^{-1} from the slope. It is hard to imagine that a long alkoxy chain such as $n_C = 13$ does not contribute at all to the entropy of transition. Consequently, another negative contribution might exist. It is natural to assume that such a contribution comes from the rest of the molecule, i.e. the 'core'. The ordinate at $n_C = 0$ is about -7 J K^{-1} mol^{-1}. This value may be identified with the entropy change necessary for the rearrangement of the 'core' while assuming that the effective core is the same as the molecular core. This gives the maximum limit of the entropy change caused by the rearrangement of the effective core in the SmC–D transition. Additional information is necessary to find a minimum limit. The study on the binary systems between ANBC–*n*-tetradecane [9] suggested that the minimum size to stabilize the D phase is larger than that of the ANBC(8) molecule. Assuming the ANBC(8) molecule to be the core, the minimum limit is estimated as -3 J K^{-1} mol^{-1}.

A similar analysis would be possible by putting the isotropic liquid as the reference state. However, it is not so straightforward. For example, the entropy of transition from the D phase to the isotropic liquid is 4.05 J K^{-1} mol^{-1} for ANBC(18) as determined in this study, while the combined entropy gain for the D–SmA and SmA–isotropic liquid transitions is 8.45 J K^{-1} mol^{-1} for ANBC(16) [8]. These two quantities, however, cannot be compared directly because their degrees of dimerization would be different. In fact, if the entropy gain integrated over the broad hump due to the dimer dissociation is added to the (combined) entropy of transition, the resulting sums amount to 18.1 J K^{-1} mol^{-1} for ANBC(16) and 16.5 J K^{-1} mol^{-1} for ANBC(18). The smaller value for the latter indicates the positive contribution of the methylene groups to the entropy of the D phase in accordance with the previous discussion using for reference the SmC phase. The small discrepancy in the resulting contribution per methylene group is rationalized by taking into account the uncertainty of drawing a baseline.

3.5. *Possibility of isostructural condensed states of matter in the D phase of ANBC and the cubic phase of BABH*

The different roles of the molecular core and the terminal chain in the D phase of ANBC has been established in the previous section. A similar analysis for the cubic phase of BABH is of real interest to examine the possibility that the two optically isotropic liquid crystalline phases are identical in nature. The entropies of transition from the cubic to the SmC phases reported for the BABHs [7] are plotted against the number of carbon atoms in one alkoxy chain (n_C) in figure 6. Contrary to the case of ANBC, the entropy of transition decreases linearly with increasing number of carbon atoms in the alkoxy chain. This indicates that the conformational degrees of freedom of the alkoxy chain are relevant to this transition, but that the methylene group has a negative contribution to the entropy of transition, in contrast to the case of ANBC. This fact means that the alkoxy chain has a higher degree of order in the SmC phase, as in the case of ANBC. Unfortunately, however, there is no spectroscopic evidence to support this conclusion. The magnitude of the slope for BABH is about -1 J K^{-1} mol^{-1}. This means that the contribution of a methylene group is -0.5 J K^{-1} mol^{-1} because a BABH molecule has two alkoxy chains. As discussed for ANBC, the upper limit of the entropy change due to the rearrangement of the 'core' is about 13 J K^{-1} mol^{-1}, while the lower limit is about 4 J K^{-1} mol^{-1}, which is obtained when the 'core' is assumed to be the molecule of BABH(8) itself.

The contribution of a methylene group to the entropy of transition from SmC to the isotropic phases is very similar in magnitude for ANBC and BABH. This clearly implies that the two isotropic phases are characterized by a very similar disorder of the terminal chains, indicating the identity of the two phases. The entropies of transition from SmC to the isotropic phases are replotted in figure 7, assuming an ANBC dimer is the constituent particle. The two lines are parallel with a slight shift. This shift is rationalized qualitatively and semi-quantitatively by considering the difference in the 'molecular' size. Since the scaling law should hold for length, the line for ANBC is expected to show a shift to the right side from that of BABH because the molecular

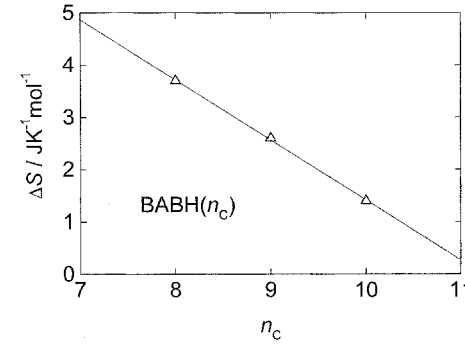

Figure 6. Entropy of transition between the cubic and SmC phases in BABH(n_C) [7].

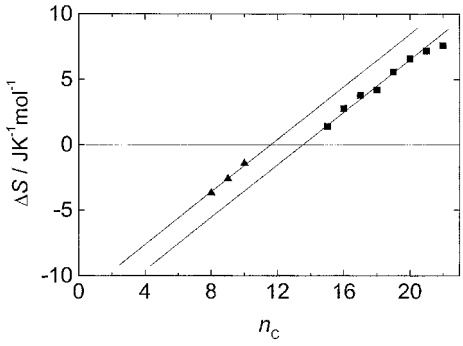

Figure 7. Entropy of transition from the SmC phase to the isotropic liquid crystalline (D of ANBC and cubic of BABH) phase per constituent particle. Filled squares, ANBC; filled triangles, BABH. The constituting particle is assumed to be a dimer for ANBC and a monomer for BABH.

core is larger for ANBC than for BABH. As seen in figure 7, the shift corresponds to about 2 in n_C and is within a reasonable range expected from the molecular size. The upper and lower bounds estimated for ANBC and BABH are also consistent.

The consistency of the treatment described above strongly suggests that the D phase of ANBC and the cubic phase of BABH are identical in nature. Assuming the identity, the upper and lower limits for the entropy change due to the 'core' are deduced to be 13 and 6 $J K^{-1} mol^{-1}$, respectively, for the transition from the isotropic (D and cubic) phase to the SmC phase.

As estimated above, contributions to the entropy of transition from the core and from the alkoxy chain have opposite signs. Since a phase with larger entropy is more stable at high temperature, the 'core' arrangement prefers the SmC structure at higher temperatures whereas the chain dynamics are favourable to the isotropic phase. As illustrated schematically in figure 8, this competition accounts for the inverted phase sequence in ANBC (SmC→D on heating) and BABH (cubic→SmC). The immiscibility of these two cubic phases derives from this inverted phase sequence, which is caused by the difference in the chian length, or the molecular size.

It seems curious that just the entropy of transition can explain the phase behaviour of ANBC and BABH, because the Gibbs energy governs the thermodynamic

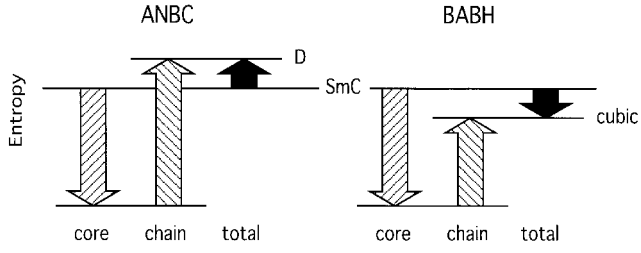

Figure 8. Inverted phase sequence and competing contributions from the molecular core and chains.

stability of phases. At the temperature of a first order phase transition, as in the present case, the Gibbs energies of two phases are equal. Consequently, the entropy and enthalpy terms are equal to each other. Since the entropy serves as a measure for a possible number of microscopic states, the entropy of transition is expected to depend linearly on the number of carbon atoms in the alkoxy chain. The enthalpy term governs the vertical position of the Gibbs energy curve on the temperature–Gibbs energy plane, i.e. the transition temperature. The disappearance of the transition for $n_C = 14$ in ANBC or $n_C = 11$ in BABH is attributed to the enthalpy term.

According to the discussion given above, there exists a possiblity that the cubic phase may appear both below and above the SmC phase in a homologous series of compounds. In this context, it is of great interest to examine what phase sequence will be realized in BABH with long chains, say, BABH(16). If the phase sequence were to become SmC–cubic in the mesogen BABH(16), the validity of the present argument would be strengthened. Such an experiment is now going on. It should be remarked here that taking into account the dependence of the transition temperature on the number of carbon atoms in a terminal chain (n_C) [9, 18], the transition temperature would show a jump when the phase sequence is reversed between cubic→SmC and SmC→cubic. As evident from the discussion so far, although the miscibility rule provides good evidence that two merged phases are identical, we should recall that immiscibility does not necessarily imply that two phases are different in nature.

4. Conclusion

The heat capacity of ANBC(18) has been measured below 500 K by adiabatic calorimetry. A crystal–crystal phase transition was discovered at 324.82 K, in addition to the known one at 337.20 K. The melting temperature of the pure substance has been determined as 399.79 K by means of the fractional melting method, while the actual crystal melted at 399.42 K. The temperature range where the D phase is thermodynamically stable has been determined as 428.07 to 464.01 K. The enthalpies and entropies of transition have been determined for all the phase transitions observed. Standard thermodynamic functions have been estimated and are tabulated at rounded temperatures.

The analysis of the entropy of transition between SmC and cubic phases definitely shows that the alkoxy chain has a higher degree of *disorder* in the cubic liquid crystalline phases of ANBC and BABH than in the SmC phase. The contribution from a methylene group to the entropy of transition is the same in both compounds, implying the identity of the isotropic phases (D and cubic)

in ANBC and BABH. A possible magnitude for the contribution of the 'core' is estimated to be negative, i.e. more *ordered* relative to SmC phase. The competition between the contributions of the 'core' and chain accounts for the inverted phase sequence in ANBC (SmC→D on heating) and BABH (cubic→SmC).

References

[1] Gray, G. W., Jones, B., and Marson, F., 1957, *J. chem. Soc.*, 393.

[2] Gray, G. W., and Goodby, J. W., 1984, *Smectic Liquid Crystals—Textures and Structures* (Glasgow and London: Leonard Hill), Chap. 4 and references therein.

[3] Demus, D., Kunicke, G., Neelsen, J., and Sackmann, H., 1968, *Z. Naturforsch.*, **23,** 84.

[4] Kutsumizu, S., Kato, R., Yamada, M., and Yano, S., 1998, *J. phys. Chem. B*, **101,** 10 666.

[5] Tansho, M., Onoda, Y., Kato, R., Kutsumizu, S., and Yano, S., 1998, *Liq. Cryst.*, **24,** 525.

[6] Schubert, H., Hauschild, J., Demus, D., and Hoffmann, S., 1978, *Z. Chem.*, **18,** 256.

[7] Demus, D., Gloza, A., Hartung, H., Hauser, A., Rapthel, I., and Wiegeleben, A., 1981, *Cryst. Res. Technol.*, **16,** 1445.

[8] Sato, A., Saito, K., and Sorai, M., 1999, *Liq. Cryst.*, **26,** 341.

[9] Saito, K., Sato, A., and Sorai, M., 1998, *Liq. Cryst.*, **25,** 525.

[10] Tardieu, A., and Billard, J., 1976, *J. Phys. (Paris) Colloq.*, **37,** C3-79.

[11] Etherington, G., Leadbetter, A. J., Wang, X. J., Gray, G. W., and Tajbakhsh, A., 1986, *Liq. Cryst.*, **1,** 209.

[12] Etherington, G., Langley, A. J., Leadbetter, A. J., and Wang, X. J., 1988, *Liq. Cryst.*, **3,** 155.

[13] Levelut, A.-M., and Fang, Y., 1991, *Colloq. Phys.*, **23,** C7-229.

[14] Levelut, A.-M., and Clerc, M., 1998, *Liq. Cryst.*, **24,** 105.

[15] Ukleja, P., Siatkowski, R. E., and Neubert, M., 1988, *Phys. Rev. A*, **38,** 4815.

[16] Yamaguchi, T., Yamada, M., Kutsumizu, S., and Yano, S., 1995, *Chem. Phys. Lett.*, **240,** 105.

[17] Morimoto, N., Saito, K., Morita, Y., Nakasuji, K., and Sorai, M., 1999, *Liq. Cryst.*, **26,** 219.

[18] Kutsumizu, S., Yamada, M., and Yano, S., 1994, *Liq. Cryst.*, **16,** 1109.

[19] Yamamura, Y., Saito, K., Saitoh, H., Matsuyama, H., Kikuchi, K., and Ikemoto, I., 1995, *J. Phys. Chem. Solids*, **56,** 107.

[20] Sorai, M., Kaji, K., and Kaneko, Y., 1992, *J. chem. Thermodyn.*, **24,** 167.

[21] Preston-Thomas, T., 1990, *Metrologia*, **27,** 107.

[22] Sorai, M., and Seki, S., 1972, *J. phys. Soc. Jpn.*, **32,** 382.

[23] Goodby, J. W., Dunmur, D. A., and Collings, P. J., 1995, *Liq. Cryst.*, **19,** 703.

[24] Smith, G. W., 1979, *Mol. Cryst. liq. Cryst.*, **49,** 207.

[25] Sorai, M., Tsuji, K., Suga, H., and Seki, S., 1980, *Mol. Cryst. liq. Cryst.*, **80,** 33.